Research Report

Practical Approach to Polymer Electrolyte Fuel Cell Modeling

Haruhiko Yamada, Yu Morimoto

固体高分子形燃料電池モデリングの実用的アプローチ

山田春彦，森本友

Abstract

A simple simulation method to predict the current distribution in a polymer electrolyte fuel cell is presented. This method combines a model for the material transport along the gas flow and through a membrane electrode gas diffusion layer assembly with experimentally determined IV (current-voltage) characteristics and water transport properties. The IV characteristics and water transport properties were measured under various gas conditions using a small cell having an electrode area of 1 cm^2. The current distribution and the humidity profile were calculated for a cell with an electrode area of 13 cm^2 for different flow patterns and stoichiometric flow ratios. The results were compared with experimental data obtained using a segmented cell and chilled-mirror hygrometers. The simulation results agreed well with the experimental data. This method gives us a rough insight into the phenomena of an operating cell and is useful for designing the cell for a membrane electrode gas diffusion layer assembly due to the simplicity of the simulation procedure.

Keywords: Polymer electrolyte fuel cell, Simulation, IV characteristic, Water transport properties, Current distribution, Humidity distribution, Experimental validation

要　旨

固体高分子形燃料電池 (PEFC) の電流分布を簡便に予測する計算手法を提案した。この手法は，ガスの流れ方向および電極接合体の厚み方向の物質移動を考慮した簡易モデルと，電極接合体の基本特性を表す実験式とを組み合せたものである。電極接合体の基本特性として，電流 - 電圧特性と水移動特性とを電極面積が1cm^2の小さなセルを用いて種々のガス条件下で測定し，実験式を導出した。この計算手法を用いて，電極面積が13cm^2のセルについてガスの流し方とガス・ストイキ比とを変えた場合の電流・湿度分布を計算し，その結果を分割セルと露点計とを用いた実験の結果と比較した。計算と実験との結果はよく一致し，ここで提案した手法の妥当性が確認できた。本手法は大きなセルの内部挙動を簡便に把握できるため，セルの設計に対して有効な手法である。

キーワード：固体高分子形燃料電池，シミュレーション，電流 - 電圧特性，水移動特性，電流分布，湿度分布，実験検証

1. Introduction

In a polymer electrolyte fuel cell (PEFC), reactant-containing gases are flown along the gas flow channels in the in-plane direction, and the reactants, hydrogen and oxygen, diffuse into catalyst layers through gas diffusion layers and are consumed in electrochemical reactions. The concentration of the reactant gases decreases downstream if the flown gas contains an inert component, such as nitrogen in the case of air. On the other hand, water produced by the electrochemical reaction is carried into the flown gases, and the concentration of water usually increases downstream. Because the changes in the concentrations of gases and water have a significant effect on the reaction rate and the proton conductivity of the membrane, the current distribution in the cell is not uniform. Therefore, in order to analyze a PEFC, it is important to obtain information on the current distribution and pursue further improvement.

The current distribution of the PEFC has been analyzed both experimentally[1, 2] and theoretically[3, 4] in previous studies. In principle, the theoretical approach with mathematical simulation is very effective for designing various PEFCs because this method can be performed without assembling an actual fuel cell. A three-dimensional simulation[5-7] has recently been developed using a computational fluid dynamic code. However, this simulation appears to be too complicated, requiring too many unknown parameters, especially for physicochemical phenomena in a membrane electrode gas diffusion layer assembly (MEGA) such as electrochemical reactions, molecular diffusion in porous media and electro-osmosis. In addition, the physicochemical models used in this simulation have not yet been verified experimentally.

In the present study, we have developed a simple simulation method to predict the current distribution and the water content profile. This method combines a simple mathematical model, which accounts for the material transport along the gas flow channel and through the MEGA, and empirical equations, which describe the IV characteristics and water transport properties of the MEGA. The validity of this method is verified by an experiment using a segmented cell and chilled-mirror hygrometers.

2. Model description

Our model, which is based on the model by Nguyen et al.,[3] is a steady-state, isothermal, quasi two-dimensional mass-transfer and electrochemical model. The model consists of two flow channels and the MEGA (**Fig. 1**). In this model the MEGA is treated as an interface having no thickness. The model accounts for the mass transport of gases and water along the gas flow channels (*x*-direction) and mass transport of water through the MEGA (*y*-direction).

The model is described in further detail as follows. The concentrations of the reactants, hydrogen and oxygen, in the flow channels change in the *x*-direction by consumption due to the electrochemical reactions. The humidities change in the *x*-direction by water production due to the electrochemical reaction and water transport in the *y*-direction. The local current density, I, is assumed to be expressed as a function of oxygen concentration (dry gas base), C_{O2}, the average of the activities of water, $a_{w,a}$ and $a_{w,c}$, and the cell voltage, V, as:

$$I = f_I\left(C_{O_2}, \frac{a_{w,a} + a_{w,c}}{2}, V\right) \quad \cdots\cdots\cdots\cdots\cdots\cdots (1)$$

where the subscripts a and c indicate the anode and cathode sides, respectively.

Water transport through the MEGA is expressed as the sum of a term proportional to the current density and a term proportional to the difference in relative humidity between the cathode flow channel and the

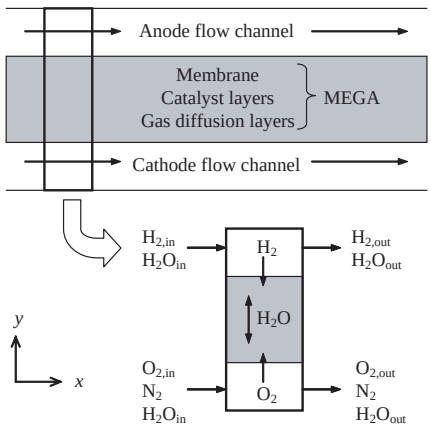

Fig. 1 Schematic diagram of modeling region.

anode flow channel. Hereafter, the former is called the gross drag coefficient, r_w, and the latter is called the gross diffusion coefficient, D_w. The parameters r_w and D_w are assumed to be functions of the average activities of water:

$$r_w = f_r\left(\frac{a_{w,a}+a_{w,c}}{2}\right) \quad \cdots\cdots\cdots\cdots\cdots\cdots (2a)$$

$$D_w = f_D\left(\frac{a_{w,a}+a_{w,c}}{2}\right) \quad \cdots\cdots\cdots\cdots\cdots\cdots (2b)$$

In the gas flow channels, condensation and evaporation of water are taken into consideration. That is, when the partial pressure of water becomes greater than the water saturation pressure, water vapor condenses and forms small droplets, the volumes of which are negligible. Similarly, when the partial pressure of water is less than the water saturation pressure, liquid water evaporates to generate water vapor.

The equations used in the model are given in **Table 1**. These equations are solved using a finite difference method.

3. Empirical expressions

The empirical expressions needed for the simulation, IV characteristics and water transport properties, were determined experimentally. A small cell with an electrode area of 1 cm^2 was used with excess flow rates in order to minimize the non-uniformity of gases and water. The MEGAs were assembled with Nafion 112 as the polymeric membrane, two carbon-supported Pt catalyst layers and two ELAT carbon cloth diffusion layers. The catalyst loadings for the anode and the cathode were 0.1 mg-Pt/cm^2 and 0.4 mg-Pt/cm^2, respectively. The measurement was conducted under the gas pressure of 2 atm abs. at 80°C.

3. 1 IV characteristics

The IV characteristics were measured under various oxygen concentrations and humidities. The oxygen concentration was controlled to be 5, 10, 15, or 20% (dry gas base) by changing the mixing ratio of oxygen and nitrogen. For the anode, pure hydrogen was supplied. The dry gas flow rates for the anode and the cathode were 70 sccm and 300 sccm, respectively. The anode and cathode gases were equally humidified with bubblers to yield a relative humidity of 16, 33, 66, or 100%. The IV characteristics were recorded using a current-sweeping method at 10 mA/s under 16 conditions.

Table 1 Governing equations.

Hydrogen	$\frac{dM_{H_2}(x)}{dx} = -\frac{h}{2F} I(x)$	(7)
Anode liquid water	$\frac{dM^l_{w,a}(x)}{dx} = \frac{M^v_{w,a}(x)}{M^v_{w,a}(x)+M_{H_2}(x)} p_a - p^{sat}_{w,a}(x)$	(8)
Anode vapor water	$\frac{dM^v_{w,a}(x)}{dx} = -\frac{dM^l_{w,a}(x)}{dx} - \frac{h\alpha(x)}{F} I(x)$	(9)
Oxygen	$\frac{dM_{O_2}(x)}{dx} = -\frac{h}{4F} I(x)$	(10)
Nitrogen	$M_{N_2,c} = M^0_{N_2,c}$	(11)
Cathode liquid water	$\frac{dM^l_{w,c}(x)}{dx} = \frac{M^v_{w,c}(x)}{M^v_{w,c}(x)+M_{O_2}(x)+M_{N_2,c}} p_c - p^{sat}_{w,c}(x)$	(12)
Cathode vapor water	$\frac{dM^v_{w,c}(x)}{dx} = -\frac{dM^l_{w,c}(x)}{dx} + \frac{h[1+2\alpha(x)]}{2F} I(x)$	(13)
Water content of membrane	$\lambda = 0.043 + 17.81 a_w - 39.85 a_w^2 + 36.0 a_w^3$	(14)
Net water transfer coefficient	$\alpha(x) = r_w(x) - \frac{F}{I(x)} D_w(x) \frac{[C_{w,c}(x) - C_{w,a}(x)]}{t_m}$	(15)
Water concentration at membrane surface	$C_w(x) = \frac{\rho_{dry}}{M_{dry}} \lambda$	(16)
Water activity	$a_w = \frac{X_w p}{p^{sat}_w}$	(17)
Vapor pressure for water	$log_{10}(p^{sat}_w) = -2.18 + 2.95\times10^{-2} T - 9.18\times10^{-5} T^2 + 1.44\times10^{-7} T^3$	(18)

Figures 2 and **3** show examples of the IV characteristics. As the oxygen concentration or relative humidity increase, the voltage and limiting current density increase.

An empirical equation was derived for each IV data by curve-fitting using the following expression proposed by Kim et al.[8]:

$$V = V_o - b\log(I) - RI - \exp(nI) \quad \ldots\ldots\ldots\ldots (3)$$

where V_o and b represent the electrode kinetic parameters for oxygen reduction, R represents the cell resistance, and the exponential term characterizes the mass transport region of the IV characteristics. In the curve-fitting, all parameters, V_o, b, R, and n, were determined using a nonlinear least squares method.

Using the determined parameters for all sets of oxygen concentration and humidity, a mathematical expression was determined as a function of oxygen concentration or gas humidity for each parameter. The obtained expressions are as follows:

$$V_o(\mathrm{mV}) = 919 + 196C_{O2} \quad \ldots\ldots\ldots\ldots\ldots\ldots (4a)$$

$$b(\mathrm{mV/decade}) = 53.4 + 6.49a_w^{-0.823} \quad \ldots\ldots\ldots (4b)$$

$$R(\Omega \cdot \mathrm{cm}^2) = 0.0934 + 0.980\exp(-5.19a_w) \quad \ldots (4c)$$

$$n(\mathrm{cm}^2/\mathrm{mA}) = 7.49 \times 10^{-4}C_{O2}^{-0.847} \quad \ldots\ldots\ldots (4d)$$

where C_{O2} and a_w are the oxygen concentration (dry gas base) and the activity of water respectively. In Figs. 2 and 3, the obtained curves are shown as solid lines. The curves agree well with the experimental data.

3. 2 Water transport properties

The gross drag of water was determined as follows. The 1-cm^2 fuel cell was operated at 0.5 A/cm^2 with H_2/air humidified equally. The relative humidities of the inlet and outlet gases were measured using chilled-mirror hygrometers. The gross drag coefficient of water was determined from the differences between the inlets and the outlets as a function of the inlet relative humidity. The gross diffusion coefficient of water was determined similarly, except that slightly different humidified H_2/air was supplied to the open-circuit cell. In these measurements, the flow rate of H_2/air = 500/500 sccm was used.

Figures 4 and **5** show respectively the gross drag coefficient of water, r_w, and the gross diffusion coefficient of water, D_w, as functions of the water content of the membrane. In these figures, the water content of the membrane was derived from the gas humidity using the sorption isotherm[9] (refer to Eq. (14) in Table 1). The negative value for the gross drag coefficient may seem unusual. However, this gross drag coefficient includes water diffusion from the cathode to the anode driven by the water concentration gradient due to water generation on the cathode. Therefore, the negative value simply means that the water diffusion from the cathode to the anode is larger than the electro-osmotic drag.[10] The gross diffusion coefficient has a maximum around the water content of 3. This agrees well with the coefficient of Motupally et al.,[11] which was extracted from the self-diffusion coefficient reported in the literature.[12] This means that the gross diffusion coefficient of the present study is nearly equal to the diffusion coefficient of water in the

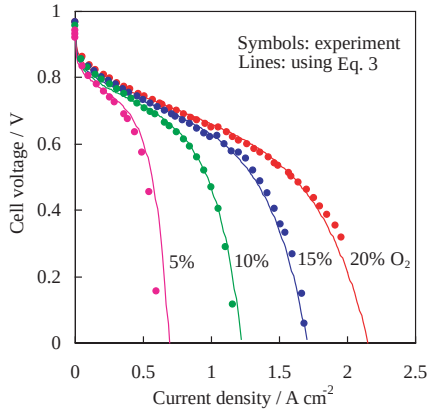

Fig. 2 Effect of O_2 concentration in the gas mixtures of O_2/N_2 on IV characteristics at RH_a=RH_c=100%.

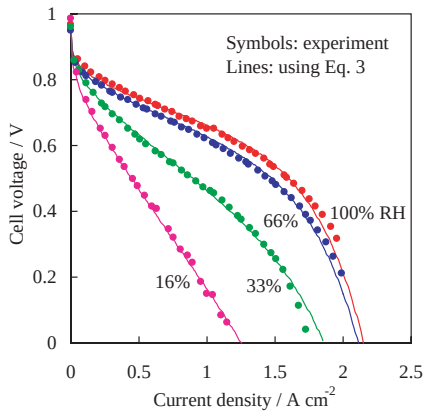

Fig. 3 Effect of relative humidity of anode and cathode on IV characteristics at 20% $O_2/(O_2+N_2)$.

membrane.

From these data, empirical equations describing the water transport properties were derived as follows:

$$r_w = 1.18\exp(-0.418\lambda) - 0.160 \quad \ldots\ldots\ldots\ldots (5)$$

$$D_w(\lambda<3) = 6.00 \times 10^{-8}\exp(1.63\lambda) \quad \ldots\ldots\ldots (6a)$$

$$D_w(\lambda\geq 3) = 5.13 \times 10^{-5}[\exp(-0.708\lambda) + 3.39 \times 10^{-2}] \quad \ldots\ldots\ldots\ldots\ldots (6b)$$

where λ is the water content of the membrane.

4. Validation

4. 1 Experimental

The current distribution was measured using a segmented cell[1)] and the gas humidity was measured at the outlets using chilled-mirror hygrometers. **Figure 6** is a schematic diagram of the 10-segmented cell. The cell has an active area of 13 cm^2 and a double-pass serpentine flow field. The same MEGA materials as the 1-cm^2 cell were used. The cell was operated under an H_2/air pressure of 2 atm abs. at 80°C. In the experiment, the gas flow pattern and the gas stoichiometric flow ratio were varied.

4. 2 Results

Figure 7 shows a comparison of the experimental and simulation results for the current density distribution for different gas flow patterns. **Figures 8** and **9** show comparisons of the experimental and simulation results for the humidity profile. The simulation results agree well with the experimental results. The simulation results of the humidity profile account well for the current distribution: the

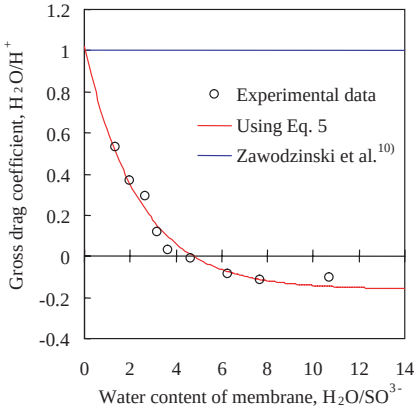

Fig. 4 Gross drag coefficient of water in Nafion membrane as a function of water content of membrane.

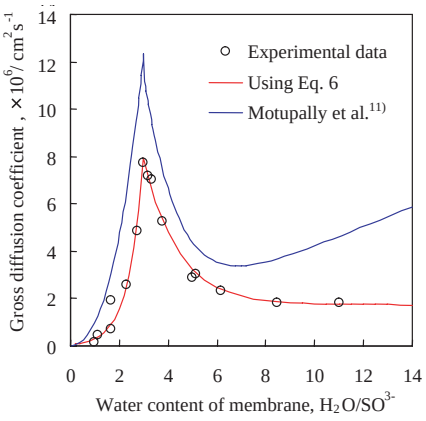

Fig. 5 Gross diffusion coefficient of water in Nafion membrane as a function of water content of membrane.

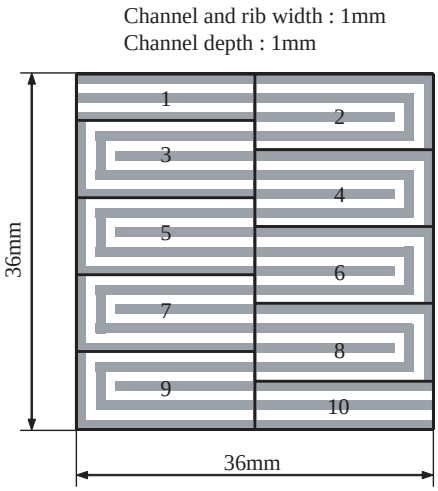

Fig. 6 Schematic diagram of the 10 segmented cell.

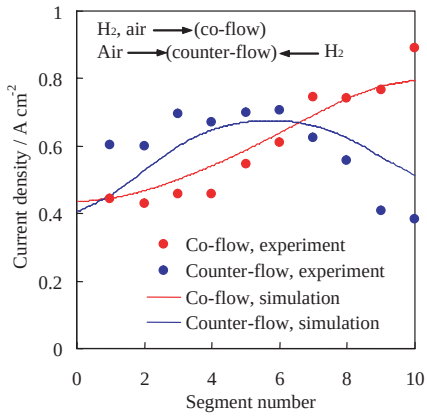

Fig. 7 Comparison of current distribution between experiment and simulation for different flow patterns at 0.6A/cm^2. The stoichiometric flow ratio is 3.3 and the inlet humidity is 33%.

high humidity makes the membrane resistance low and the current density high. In this high-stoichiometric-flow condition, oxygen concentration does not have a significant influence on the current density. **Figure 10** shows the IV characteristic of the simulation compared to that of the experiment. The simulation results agree well with the experimental data.

Figure 11 shows a comparison between simulation and experimental results for the current distribution for different gas stoichiometric flow ratios. In the low-stoichiometric-flow condition, the current density shows the effect of low oxygen concentration downstream. In this case, again, the simulation results agree well with the experimental data.

5. Conclusions

We have proposed a simulation method to predict the current distribution in a real PEFC. Rather than using theoretical equations, the proposed method employs overall empirical equations determined by small-cell experiments for physicochemical phenomena such as electrochemical reactions, molecular diffusion in a polymer or porous media and electro-osmosis. Therefore, uncertainties on

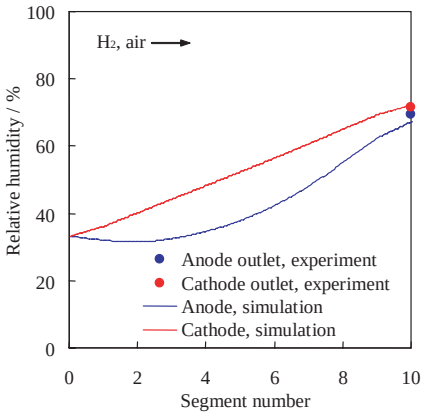

Fig. 8 Calculated humidity profile and measured humidity at outlet at 0.6A/cm^2 for co-flow. The stoichiometric flow ratio is 3.3 and the inlet humidity is 33%.

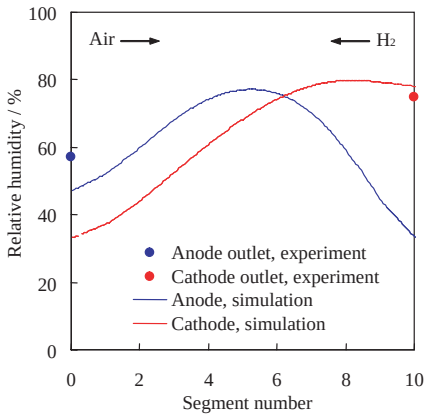

Fig. 9 Calculated humidity profile and measured humidity at outlet at 0.6A/cm^2 for counter-flow. The stoichiometric flow ratio is 3.3 and the inlet humidity is 33%.

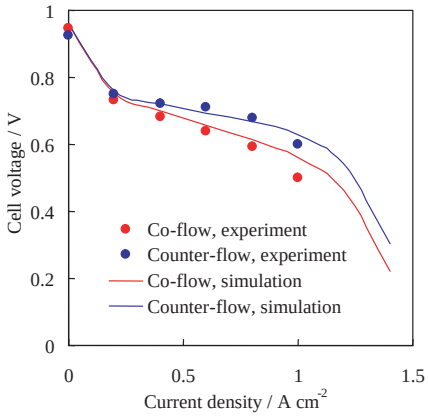

Fig. 10 Comparison of IV characteristic between simulation and experiment for both gas flow. The stoichiometric flow ratio is 2 at 1A/cm^2 and the inlet humidity is 33%.

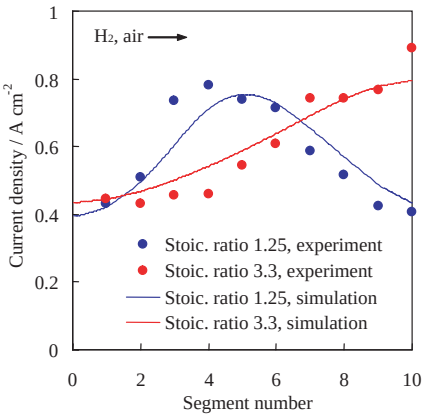

Fig. 11 Comparison of current distribution between simulation and experiment for different stoichiometric flow ratios. The stoichiometric flow ratio is 3.3 and the inlet humidity is 33%. The inlet humidity is 33% and the flow pattern is co-flow.

physicochemical models and their parameters can be avoided, and the effects of engineering and designing, such as flow patterns and operation conditions, can be clarified. For this reason, we believe that this approach will be highly useful in practical application.

A drawback of this approach is that the effects of material properties and microstructures cannot be separately recognized because these effects are combined in the empirical equations. Therefore, it is difficult to obtain hints for improving the materials and microstructures. However, such improvements require that the physicochemical phenomena in PEFCs be fully understood and that their models be verified experimentally using a small cell while avoiding engineering and designing effects.

List of Symbols

a_w : activity of water
b : tafel slope/mV decade^{-1}
Co_2 : oxygen molar fraction in dry O_2/N_2 gas mixtures
C_w : concentration of water/mol cm^{-3}
D_w : gross diffusion coefficient of water/cm^2 s^{-1}
F : Faraday constant/C mol^{-1}
h : MEGA width/cm
I : local current density/A cm^{-2}
M : molar flow rate/mol s^{-1}
M_{dry} : equivalent weight of a dry membrane/g mol^{-1}
n : mass transport parameter
p : pressure/atm
R : cell resistance/Ω cm^2
r_w : gross drag coefficient of water
T : temperature/^{o}C
t_m : membrane thickness/cm
V : cell voltage/V
V_0 : open circuit voltage/V
X : molar fraction
x : direction along the gas channel length/cm

Greek

α : net water transfer coefficient per proton
ρ_{dry} : density of a dry membrane/g cm^{-3}
λ : water content of membrane

Subscripts and superscripts

a : anode
c : cathode
H_2 : hydrogen
l : liquid
N_2 : nitrogen
O_2 : oxygen
sat : saturation
v : vapor
w : water
0 : initial condition

References

1) Morimoto, Y., Suzuki, T. and Yamada, H. : The Electrochem. Soc. Meet. Abstr., MA2002-2 (2002), No. 816, ECS
2) Mench, M. M., Wang, C. Y. and Ishikawa, M. : J. Electrochem. Soc., **150**(2002), A1052
3) Nguyen, T. V. and White, R. E. : J. Electrochem. Soc., **140**(1993), 2178
4) Gurau, V., Liu, H. and Kakac, S. : AIChE J., **44**(1998), 2410
5) Um, S. and Wang, C. Y. : J. Power Sources, **125**(2004), 40
6) Berning, T., Lu, D. M. and Djilali, N. : J. Power Sources, **106**(2002), 284
7) Dutta, S., Shimpalee, S. and Van Zee, J. W. : J. Appl. Electrochem., **30**(2000), 135
8) Kim, J., Lee, S. M. and Srinivasan, S. : J. Electrochem. Soc., **142**(1995), 2670
9) Springer, T. E., Zawodzinski, T. A. and Gottesfeld, S. : J. Electrochem. Soc., **138**(1991), 2334
10) Zawodzinski, T. A., Davey, J., Valerio, J. and Gottesfeld, S. : Electrochim. Acta, **40**(1995), 297
11) Motupally, S., Becker, A. J. and Weidner, J. W. : J. Electrochem. Soc., **147**(2000), 3171
12) Zawodzinski, T. A., Neeman, M., Sillerud, L. O. and Gottesfeld, S. : J. Phys. Chem., **95**(1991), 6040

(Report received on Jul. 19, 2004)

Haruhiko Yamada
Year of birth : 1959
Division : Fuel Cell System Lab.
Research fields : Electrochemistry, Fuel cell
Academic society : Electrochem. Soc. Jpn.

Yu Morimoto
Year of birth : 1957
Division : Fuel Cell System Lab.
Research fields : Electrochemistry, Fuel cell
Academic degree : Ph. D.
Academic society : Electrochem. Soc., Electrochem. Soc. Jpn.